

Mechanisms of Guanosine Triphosphate Hydrolysis by Ras and Ras-GAP Proteins as Rationalized by Ab Initio QM/MM Simulations

Bella L. Grigorenko,¹ Alexander V. Nemukhin,^{1*} Maria S. Shadrina,¹ Igor A. Topol,² and Stanley K. Burt²

¹Department of Chemistry, M.V. Lomonosov Moscow State University, Moscow, 119992, Russian Federation

²Advanced Biomedical Computing Center, SAIC Frederick, National Cancer Institute at Frederick, Frederick, Maryland 21702-1201

ABSTRACT The hydrolysis reaction of guanosine triphosphate (GTP) by p21^{ras} (Ras) has been modeled by using the ab initio type quantum mechanical-molecular mechanical simulations. Initial geometry configurations have been prompted by atomic coordinates of the crystal structure (PDBID: 1QRA) corresponding to the prehydrolysis state of Ras in complex with GTP. Multiple searches of minimum energy geometry configurations consistent with the hydrogen bond networks have been performed, resulting in a series of stationary points on the potential energy surface for reaction intermediates and transition states. It is shown that the minimum energy reaction path is consistent with an assumption of a two-step mechanism of GTP hydrolysis. At the first stage, a unified action of the nearest residues of Ras and the nearest water molecules results in a substantial spatial separation of the γ -phosphate group of GTP from the rest of the molecule (GDP). This phase of hydrolysis process proceeds through the low barrier (16.7 kcal/mol) transition state TS1. At the second stage, the inorganic phosphate is formed in consequence of proton transfers mediated by two water molecules and assisted by the Gln61 residue from Ras. The highest transition state at this segment, TS3, is estimated to have an energy 7.5 kcal/mol above the enzyme-substrate complex. The results of simulations are compared to the previous findings for the GTP hydrolysis in the Ras-GAP (p21^{ras}-p120^{GAP}) protein complex. Conclusions of the modeling lead to a better understanding of the anticatalytic effect of cancer causing mutation of Gln61 from Ras, which has been debated in recent years. *Proteins* 2007;66: 456–466. © 2006 Wiley-Liss, Inc.

Key words: G-proteins; Ras; Ras-GAP; GTP hydrolysis; QM/MM modeling

INTRODUCTION

The mechanism of hydrolysis of guanosine triphosphate (GTP) by G-proteins, leading to guanosine diphosphate (GDP) and inorganic phosphate (Pi), which constitutes one of the most important enzymatic reactions responsible

for normal and tumorigenic cellular signal transduction, continues to remain a subject of active debates.^{1–11} The most recent publications by Wittinghofer,¹¹ Li and Zhang,¹⁰ and Pasqualato and Cherfils¹² comprehensively review the subject summarizing advances from structural, kinetic, spectroscopic, and theoretical studies. Two types of the reaction mechanism are usually compared as differentiated by the nature of a transition state. On one extreme, a fully dissociative transition state for the GTP hydrolysis is represented by an intermediate that shows bond cleavage between the γ -phosphate group and GDP. On the other extreme, a fully associative transition state is represented by a penta-coordinated intermediate that shows no β - γ bridge bond cleavage but significant amount of bond formation between the incoming lytic water molecule and the γ -phosphate of GTP. It should be noted that none of the available experiments can determine whether the mechanism is associative or dissociative.¹³ Another popular model suggests that the substrate GTP itself, specifically γ -phosphate group of GTP, serves as the general base in its own hydrolysis.⁹ Modeling the catalytic mechanism of the GTP hydrolysis by Ras and Ras-GAP in the complete enzyme has been performed by Warshel and coworkers^{14–20} by using the empirical valence bond (EVB) methodology.²¹ In this approach, the diagonal elements of the EVB Hamiltonian (the diabatic energies) describe the energies of valence bond electronic structures, while the different resonant structures are mixed by off-diagonal elements. All EVB matrix elements are calibrated using experimental information or ab initio quantum chemistry calculations. Reference 19 describes simulations of the GTP hydrolysis reaction in Ras-GAP along the alternative associative and dissociative paths by relying on the EVB

Grant sponsor: Russian Foundation for Basic Researches; Grant number: 04-03-32008; Grant sponsor: Russian Federal Agency of Sciences and Innovation for BLG; Grant number: 02.442.11.7444; Grant sponsor: National Cancer Institute, National Institutes of Health; Grant number: NO1-CO-12400.

*Correspondence to: Alexander V. Nemukhin, Department of Chemistry, M.V. Lomonosov Moscow State University, Moscow, 119992, Russian Federation. E-mail: nemukhin@ncisgi.ncifcrf.gov or anem@lcc.chem.msu.ru

Received 29 March 2006; Revised 4 August 2006; Accepted 22 August 2006

Published online 8 November 2006 in Wiley InterScience (www.interscience.wiley.com). DOI: 10.1002/prot.21228

parameters used in previous estimates for the Ras-catalyzed reaction¹⁴ and those partly fitted to the results of ab initio quantum chemistry calculations for the methyl monophosphate ester hydrolysis in aqueous solution.¹⁵ The interactions between the EVB atoms and the rest of the system were represented by the ENZYFIX force field parameters.²² These simulations resulted in a conclusion that the reaction most likely corresponded to an associative mechanism. In Ref. 20 only associative type mechanism was assumed in simulations, and the EVB matrix elements were noticeably reparameterized. The authors²⁰ reported the estimated free energies of the first transition state, the penta-coordinated intermediate, and the second transition state for the GTP hydrolysis in water (20.0, 18.4, and 27.9 kcal/mol), in Ras (15.2, 11.9, and 23.2 kcal/mol), and in Ras-GAP (16.1, 9.0, and 13.5 kcal/mol), which were consistent with the values converted from the experimental rate constants ($4.7 \times 10^{-4} \text{ s}^{-1}$ in Ras and 19 s^{-1} in Ras-GAP) by using a simple formula of the transition state theory: 27.5 (water), 22.2 (Ras), and 15.9 kcal/mol (Ras-GAP).

Futatsugi et al.²³ used the cluster (or supermolecular) approach to model the hydrolysis reaction in Ras at the ab initio quantum chemistry level. Following the results of preliminary energy minimization by molecular mechanics (MM) methods for the system based on the Ras-type 121p PDB-structure, the authors selected a highly simplified molecular cluster (including diphosphate as a model for GTP, fragments of Lys16, Ser17, Thr35, and a water molecule) to represent the active site of the enzyme. Ab initio (SCF/6-31G(d,p)) intrinsic reaction coordinate (IRC) calculations, with several geometry constraints, were used to construct the energy reaction pathway. These calculations suggested that the hydrolysis reaction in a cluster environment proceeds in one step with an activation energy of 42 kcal/mol. The authors promoted the so-called proton-relay mechanism, since in their calculations the initially charged residue Lys16 donated the proton to γ -phosphate facilitating the reaction. Such an approach, and the resulting conclusions, was criticized in Ref. 20 on the grounds that Futatsugi et al. actually studied a gas phase system and the appearance of the unstable lysine was an artifact of the model. Nevertheless, in a subsequent publication, Futatsugi and Tsuda²⁴ explored the idea of a crucial role of Lys16 in the GTP \rightarrow GDP hydrolysis while interpreting the results of their molecular dynamics (MD) simulations of the Gly12 \rightarrow Val mutant of Ras. In another paper²⁵ of the same research group, the proton relay mechanism of GTP hydrolysis was considered in attempts to model the hydrolysis reaction GTP \rightarrow GDP by the Gi α 1 protein, the latter being a kind of a GTPase-activating protein. Again, a cluster model was selected for quantum chemistry calculations at the SCF and DFT levels, and detachment of a hydrogen atom from lysine, this time to the O $_{\beta}$ atom of phosphate, was considered as a key component of the reaction mechanism. The estimated activation energy amounted to 35 kcal/mol.

Unrealistic activation energies reported in Ref. 23–25 which are inconsistent with the observed reaction rates

prompt us to exclude from consideration the reaction mechanisms discussed in these papers.

Cavalli and Carloni²⁶ performed simulations of GTP hydrolysis in the Cdc42/Cdc42GAP protein complex (a relative of the Ras-GAP system) by using the Car-Parrinello MD calculations. By analyzing relatively short trajectories, the authors concluded that the attacking water molecule was highly polarized by the active site and donated a proton to Gln61, whereas the proton transfer to γ -phosphate was highly unfavorable. Therefore, the authors rejected the mechanism of substrate assisted catalysis for GTP hydrolysis.

Klöhn et al.²⁷ applied the combined density functional (DFT) and MM method to characterize vibrational spectra and the mode of binding of GTP to Ras. Consistent with experimental findings and discussions presented in Ref. 19 these simulations pointed out that the charge shift toward the β -phosphate should be catalytic for the hydrolysis for any type of the reaction mechanism.

Essential dynamics analysis based on the averaged structural features observed in the MD simulations of the equilibrated protein complex Ras-GTP was used by Soares et al.²⁸ to hypothesize the reaction mechanism. The authors offered a catalytic model aimed to explain the importance of Gln61 in the GTPase activity of Ras. Their proton-shuttle model assumed active participation of two water molecules one of which should be positioned in an appropriate orientation for proton transfers by Gln61. As stated by the authors the feasibility of such mechanism would require the determination of activation energies of the protonation reactions that were “beyond the scope of the study.”²⁸

In previously described simulations of GTP hydrolysis in the Ras-GAP protein complex^{29,30} we applied quantum chemical methods and an ab initio type version^{31–35} of the combined quantum mechanics–molecular mechanics (QM/MM) theory,^{36–38} concluding that the low-energy reaction profile was consistent with the two step reaction mechanism. The first step refers to the cleavage of the O $_{\beta}$ –P $_{\gamma}$ bond and separation of the γ -phosphate group from the rest of the triphosphate moiety. At the second step, the Pi is formed in consequence of proton transfers via the nearby molecular groups involved in the hydrogen bond network. We agree with the comment formulated in Ref. 39 that “. . . it would be crucial to examine the corresponding result [proposal of a metaphosphate intermediate in the Ras-GAP complex] in related systems as Ras alone. . . .”³⁹ Therefore, the present contribution is devoted to modeling the reaction GTP + H $_2$ O \rightarrow GDP + Pi in the Ras (p21^{Ras}) protein by using precisely the same QM/MM methodology as in our previous calculations for the Ras-GAP system³⁰ and in modeling the methyl triphosphate hydrolysis in water.⁴⁰

SIMULATIONS

For calculations of the reaction energy profile we use the ab initio type QM/MM method based on the theory of effective fragment potentials (EFP).³¹ Consistent with

previous calculations,^{29,30,40} all phosphate groups of GTP, the catalytic water molecule, and the neighboring molecular groups, here the side chain of Gln61 and one more water molecule, are assigned to the QM part as clarified later.

The effective fragment potential based QM/MM technique is an approach which allows one to perform calculations close to an ab initio treatment of the entire molecular system.³¹ In this scheme, molecular groups assigned to the MM part are represented by effective fragments which contribute their electrostatic potentials expanded up to octupoles to the quantum Hamiltonian. These one-electron electrostatic potentials as well as contributions from interactions of effective fragments with the QM region are obtained in preliminary quantum chemical calculations by using ab initio electron densities.³¹ The exchange-repulsion potentials to be combined with the electrostatic and polarizability terms are also created in preliminary ab initio calculations. Thus, all empirical parameters are entirely within the MM subsystem. In the original EFP based approach,³¹ interactions between solvent molecules are computed as EFP–EFP interactions. In our flexible effective fragment version^{32–35} we replace the EFP–EFP terms by the force field parameters, here from the AMBER library.⁴¹ The computer program created on the base of the GAMESS(US)⁴² (more specifically, its Intel-specific version, PC GAMESS⁴³) quantum chemistry package and molecular modeling system TINKER⁴⁴ was used in simulations.

Simulations included scans of the composite multidimensional QM/MM potential energy surface in the regions where chemical bonds or hydrogen bonds could be cleaved or formed. As a result, the basins around presumable stationary points were specified for more careful calculations of the local minima or saddle points. All stationary points considered below were located by unconstrained minimizations (for local minima) or by constrained minimizations (for saddle points) of the QM/MM energy. Locations of the saddle points or, in other words, of transition states (TS) were performed based on the following criterion: the gradient of the constrained internal coordinate along an assumed reaction path must change its sign at this point. The polarized “LANL2DZdp ECP” basis set (and the corresponding pseudopotential for phosphorus)⁴⁵ was used for all atoms except magnesium. For the latter, the standard 6–31 basis set was employed. Since the reaction profile for the Ras-GAP protein complex was computed in the SCF approximation, the same approach was applied in the present application.

It should be noted that multiple minimum energy points could be located in geometry optimizations. We attempted to overcome this difficulty by performing in each case numerous selections of the starting sets of coordinates for minimization until the lowest energy was reached under the condition that hydrogen bond network in the immediate vicinity of GTP retains its structure.

The initial positions of the atoms of the Ras-GTP complex were prompted by two crystal structures from the

Protein Data Bank.⁴⁶ The structure 1QRA was determined at the 1.6 Å resolution by Scheidig and co-authors⁴⁷ for the complex formed between p21^{ras} and GTP using a combination of photolysis of an inactive GTP precursor and rapid freezing at 100 K. The structure 5P21 was solved at the 1.35 Å resolution by Pai and coworkers for human H-Ras (p21^{ras}) bound to the GTP analog (GppNHp) at 277 K.⁴⁸ The largest deviations between the structures Ras-GTP (100 K) and Ras-GppNHp (277 K) were observed around the loop of switch II region. However, this loop with residues 60–64 and the start of helix α 2 with residues 65–67 were the most poorly defined regions for the Ras-GppNHp structure, as reflected by the B-factor plot.⁴⁸ As revealed, in particular, by our preliminary MD simulations, these particular regions are very flexible and it is reasonable to agree with the proposals formulated in both works^{47,48} that “catalytically active conformation” corresponds to such orientation of the Gln61 side chain, which helps to position the lytic water molecule, but it is not in direct contact with the γ -phosphate group of GTP.

Our model system QM/MM for calculations included the following amino acid residues from Ras: Val7 Val8 Val9 Gly10 Ala11 Gly12 Gly13 Val14 Gly15 Val14 Gly15 Lys16 Ser17 Ala18 Leu19 Thr20 Ile21 Gly22 Leu23 Ile24 Gln25 Asn26 His27 Phe28 Val29 Asp30 Glu31 Tyr32 Asp33 Pro34 Thr35 Ile36 Glu37 Asp38 Ser39 Tyr40 Arg41 Ile55 Leu56 Asp57 Thr58 Ala59 Gly60 Gln61 Glu62 Glu63 Tyr64 Ser65 Arg68 Tyr71 Leu79 Cys80 Val81 Phe82 Ala83 Ile84 Asn85 Asn86 Thr87 Lys88 Ser89 Phe90 Glu91 Aps92 Ile93 His94 Glu95 Tyr96 Arg97 Leu113 Val114 Gly115 Asn116 Lys117 Cys118 Asp119 Leu120 Ala121 Glu143 Thr144 Ser145 Ala146 Lys147 Thr148 Arg149 Gly150. All residues Lys and Arg were assumed positively charged (protonated), while Asp and Glu were considered negatively charged (unprotonated). The QM/MM model system also included 105 explicit water molecules, the magnesium cation, Mg²⁺, and the unprotonated GTP molecule. A total amount and initial positions of water molecules as well as selection of particular amino acid residues were inspired by the requirement that GTP must be completely buried inside “solvent” shells of peptide groups and water molecules. Figure 1 illustrates a general view on the model system.

RESULTS

Enzyme–Substrate (ES) Complex

In pilot calculations, several partitioning schemes to the QM and MM subsystems were tested. In all cases three phosphate groups of GTP, magnesium cation, two water molecules, and side chain of Gln61 were assigned to the QM part, but number of water molecules described either by effective fragments or explicitly at the ab initio level was varied. As mentioned earlier, two starting sets of initial coordinates of heavy atoms were considered for energy minimization prompted by the 1QRA and 5P21 structures. In the latter case the bridg-

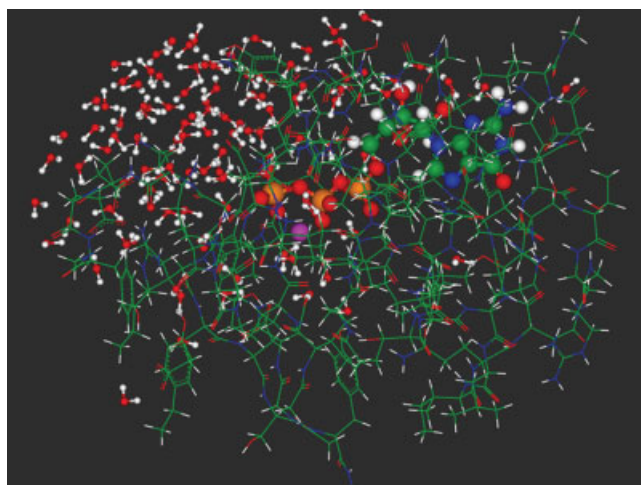


Fig. 1. The model system for QM/MM calculations. Carbon atoms are shown in green, oxygen in red, nitrogen in blue, magnesium in magenta, phosphorus in dark yellow. Large balls and sticks distinguish the GTP moiety and magnesium cation. Smaller balls and sticks depict water molecules while lines show the peptide chains.

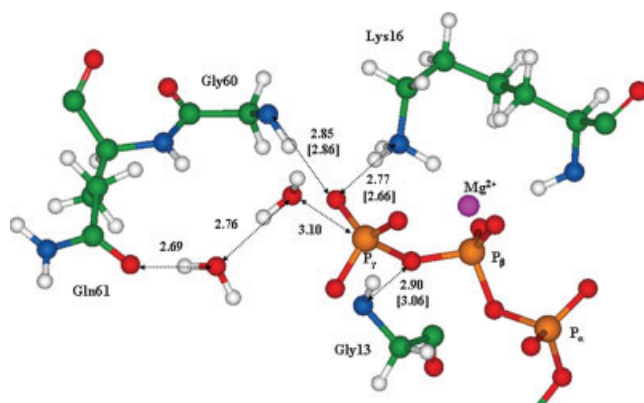
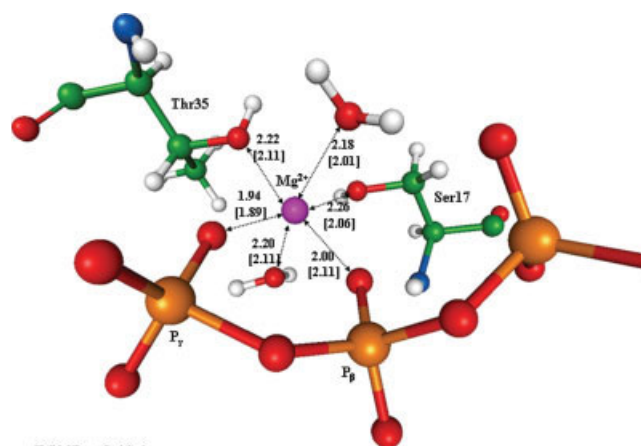


Fig. 2. A fraction of the computed geometry configuration of the ES complex. In calculations, the phosphate groups of GTP, magnesium cation, side chain of Gln61, and two water molecules were included to the QM subsystem. The distances between heavy atoms are shown in angstroms. The values in brackets refer to the 1QRA structure.⁴⁷

ing NH group in GppNHp was replaced by the oxygen atom and the loop of the switch II region was shifted to the position basically consistent with the 1QRA structure. In all attempts we arrived to the same QM/MM minimum energy configuration fragments of which are shown in Figures 2 and 3.

Figure 2 illustrates an arrangement of the nearest amino acid residues and water molecules around GTP in the ES complex. The shown distances (in Å) between heavy atoms without brackets were obtained in QM/MM optimization of all internal coordinates in the QM part, which included three phosphate groups of GTP, magnesium cation, side chain of Gln61, and two water molecules displayed in Figure 2, and the coordinates of vast majority of effective fragments representing the MM part (only terminal peptide groups were kept frozen as in the crystal structures). The distances in square brackets refer to



RSMD = 0.13 Å

Fig. 3. A fraction of the computed geometry configuration of the ES complex showing coordination shell of magnesium cation. The distances between heavy atoms are specified in angstroms. The values in brackets refer to the 1QRA structure.⁴⁷

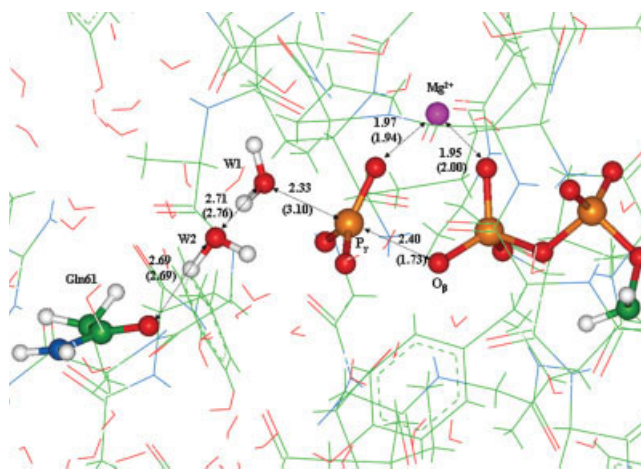


Fig. 4. Geometry configuration of the first transition state TS1 showing atoms of the quantum part in the ball and stick representation. Distances between heavy atoms (in Å) without parentheses correspond to the TS1 structure, distances in parentheses correspond to the geometry of the previous stationary point, the ES complex (Figs. 2 and 3).

the 1QRA structure. One can see that positions of the Lys16, Gly60, and Gly13 residues relative to GTP are in excellent agreement with the experimental data in spite of the point that coordinates of these residues are optimized as those of effective fragments (MM part) while coordinates of GTP are optimized in QM calculations.

Although it is difficult to compare optimized positions of two water molecules displayed in Figure 2 to positions of water molecules W175 and W189 in 1QRA,⁴⁷ consideration of their arrangements relative to Gln61 and γ -phosphate provides a certain support to the hypothesis of the “two-water model” proposed by Scheidig et al.⁴⁷ This issue will be discussed in details in the forthcoming section.

Figure 3 shows another fraction of the computed geometry configuration of the ES complex displaying coordination shell of magnesium cation. The distances between

heavy atoms are specified in angstroms. The values in brackets refer to the 1QRA structure. We stress that the phosphate groups of GTP and Mg^{2+} were assigned to the QM part but coordinates of all other molecular groups displayed in Figure 3 were optimized as effective fragments of the MM part. Again an excellent agreement with the experimental structure is seen. A quantitative estimate of the deviation of the computed interatomic distances from the experimental ones gives the RMSD value of 0.13 Å, if we consider the corresponding pairs without and with square brackets shown in Figures 2 and 3.

Another important comparison may be performed for the distances between P_γ and the bridging O_β atom. The value for the $P_\gamma-O_\beta$ distance in Ras was obtained in our QM/MM calculations as 1.73 Å, while the corresponding distances for methyl triphosphate in water clusters were estimated as 1.69 Å,⁴⁰ and for GTP in the Ras-GAP protein complex as 1.78 Å.³⁰ The change in the $P_\gamma-O_\beta$ bond length of GTP in Ras and in water found in our calculations is well consistent with the change reported in QM/MM calculations of Klähn et al.²⁸: 1.74 vs 1.70 Å. Binding of GTP by the Ras protein leads to a weakening of the $P_\gamma-O_\beta$ bond compared to aqueous solution.

Reaction Pathway

Calculations of the minimum energy profile for the hydrolysis reaction were performed with the same assignment of molecular groups to the QM part: namely, all phosphate species of GTP, magnesium cation, a fragment of side chain of Gln61, and two water molecules shown in Figure 2 were treated as quantum particles (32 atoms described by 326 basis functions), while the remaining molecular groups were included to the 1464-atomic MM subsystem represented by 443 effective fragments.

As in our previous QM/MM calculations,^{30,40} the reaction coordinate for the first phase of hydrolysis was selected as the distance from P_γ to the oxygen atom of the nucleophilic water molecule. By gradually decreasing this distance from its value in ES (3.10 Å) and optimizing each time all other geometry parameters of the QM/MM model system we succeeded to locate the first transition state TS1 (see Fig. 4), which separated the ES complex (see Figs. 2 and 3) and the first intermediate INT1 (see Fig. 5). Geometry configuration of TS1 shown in Figure 4 is characterized by the almost planar PO_3 moiety spatially well separated from GDP (the $P_\gamma-O_\beta$ distance constitutes 2.40 Å compared to the value of 1.73 Å in ES) while the assisting water molecules, W1 and W2, remain practically unaltered: O–H bond lengths in W1 and W2 constitute 0.95–0.97 Å. According to QM/MM calculations the energy of TS1 relative to the ES level is 16.7 kcal/mol.

In the INT1 structure (see Fig. 5), representing the local minima on the composite QM/MM potential energy surface, the $P_\gamma-O_\beta$ distance amounts to 3.16 Å, while the O_1-P_γ distance from lytic water molecule W1 to γ -phosphate decreases to 1.81 Å. Two water molecules, W1

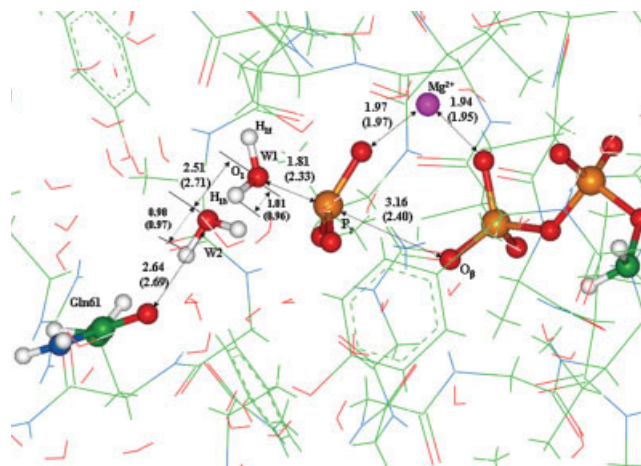


Fig. 5. Geometry configuration of the first intermediate INT1 showing atoms of the quantum part in the ball and stick representation. Distances (in Å) without parentheses correspond to the INT1 structure and distances in parentheses correspond to the geometry of the previous transition state, TS1 (see Fig. 4). [Color figure can be viewed in the online issue, which is available at www.interscience.wiley.com.]

and W2, are getting closer. The QM/MM energy at this point is 8.1 kcal/mol above the ES level and 8.6 kcal/mol lower than that of TS1.

Conformation of the metaphosphate unit PO_3 in the INT1 structure, in which the $P_\gamma-O_\beta$ bond is apparently cleaved (see Fig. 5), is stereochemically inverted relative to conformation of the γ -phosphate group of GTP in the ES structure, and as such, it is prepared to the nucleophilic attack of O_1H_{1r} hydroxyl group from the lytic water molecule W1 (see Fig. 5). Therefore, for the next segment of the reaction path, we selected the O_1-H_{1b} distance as a reaction coordinate. By gradually increasing this distance from its value in INT1 (1.01 Å) and optimizing each time all other geometry parameters of the QM/MM model system we found the structure corresponding to the second intermediate INT2 displayed in Figure 6.

Two local minimum energy structures, INT1 and INT2, of course, are separated by a potential barrier TS2. We scanned the corresponding region of the configurational space and found that the height of TS2 must be very low relative to INT1, not higher than 2 kcal/mol.

The structure of INT2 seems fairly peculiar. Apparently, the HPO_4^{2-} particle is created from metaphosphate and the hydroxyl (O_1-H_{1r}) from the water molecule W1, since the O_1-P_γ distance is now 1.62 Å. A transient species of Gln61 with a captured proton originally from the water molecule W2 is energetically more preferable than another possible transient species H_3O^+ . The energy of INT2 configuration is -1.4 kcal/mol relative to the ES level and 6.7 kcal/mol lower than that of INT1.

For the next move, we considered the $O(\text{Gln61})-H_{2b}$ distance as the reaction coordinate. By increasing this distance from the initial value 0.98 Å in INT2 and optimizing all other geometry parameters we located the third transition state TS3 (see Fig. 7) separating INT2

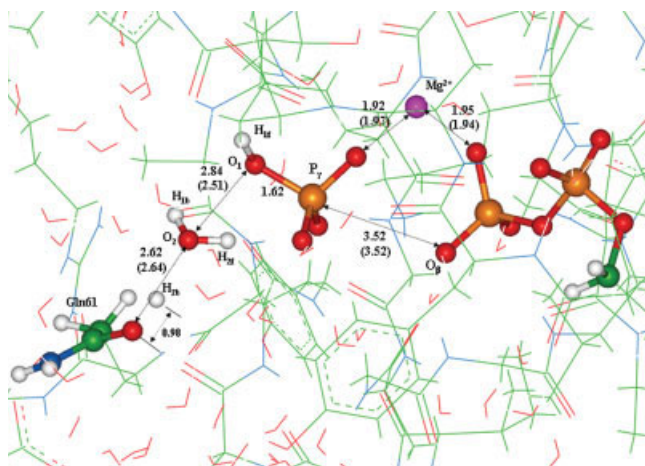


Fig. 6. Geometry configuration of the second intermediate INT2 showing atoms of the quantum part in the ball and stick representation. Distances (in Å) without parentheses correspond to the INT2 structure and distances in parentheses correspond to the geometry of the previous intermediate INT1 (see Fig. 5). [Color figure can be viewed in the online issue, which is available at www.interscience.wiley.com.]

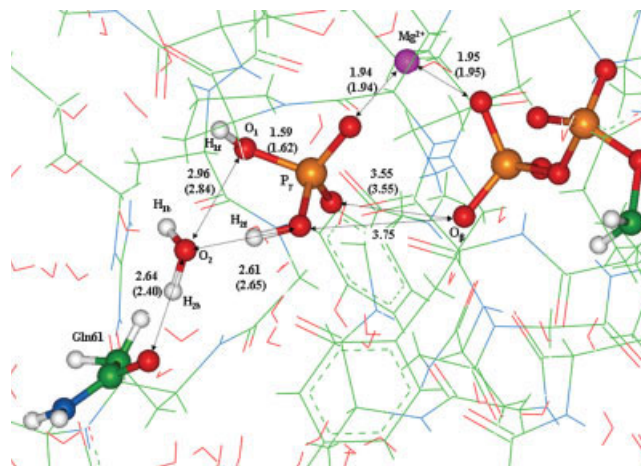


Fig. 8. Geometry configuration of the reaction products (PR1) showing atoms of the quantum part in the ball and stick representation. Distances (in Å) without parentheses correspond to the PR1 structure and distances in parentheses correspond to the geometry of the previous structure TS3 (see Fig. 7). [Color figure can be viewed in the online issue, which is available at www.interscience.wiley.com.]

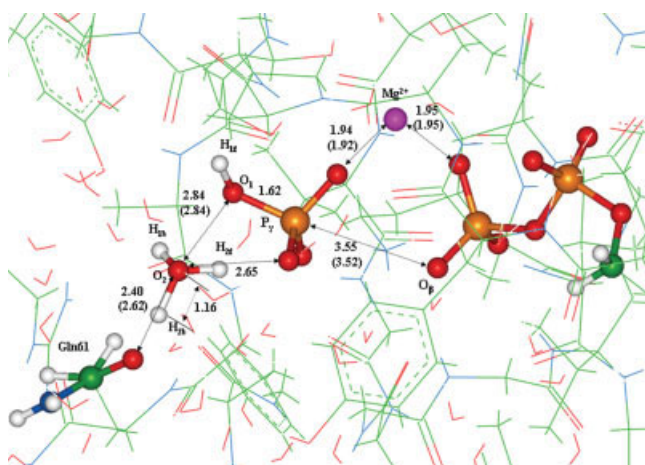


Fig. 7. Geometry configuration of the third transition state TS3 showing atoms of the quantum part in the ball and stick representation. Distances (in Å) without parentheses correspond to the TS3 structure and distances in parentheses correspond to the geometry of the previous intermediate INT2 (see Fig. 6). [Color figure can be viewed in the online issue, which is available at www.interscience.wiley.com.]

and products. The transient H_3O^+ species with a slightly elongated distance $\text{O}_2\text{—H}_{2b}$ is apparently a feature of the TS3 structure. The energy of TS3 is 7.5 kcal/mol relative the ES level and 8.9 kcal/mol above the INT2 level.

A downright descent from TS3 allowed us to arrive to configuration corresponding to the products (more precisely, enzyme-product complex) GDP and H_2PO_4^- which is illustrated in Figure 8. We designate this structure as PR1 as clarified later.

We would be satisfied with the results of simulations by standing at this point since the geometry configuration shown in Figure 8 seems fairly rationale one, and the energy of the product state PR1 is lower than the

energy of the ES complex by a reasonable amount 6.8 kcal/mol. However, after getting acquainted with the paper¹² by Pasqualato and Cherfills entitled “Crystallographic evidence for substrate-assisted GTP hydrolysis by a small GTP binding protein,” we reconsidered the final destination of the GTP hydrolysis reaction in Ras. Pasqualato and Cherfills reported the high resolution crystal structure of a small G protein, Rab11, solved in a complex with GDP and Pi (PDB accession code 1OIX). The authors state¹² that “a Pi oxygen and the GDP cleaved oxygen are located less than 2.5 Å apart suggesting that they share a proton, likely in the form of low-barrier hydrogen bond. This implies that the γ -phosphate of GTP was protonated; hence, that GTP acts as a general base”. In the product structure obtained in our simulations for GTP hydrolysis in Ras, the Pi oxygen and the GDP cleaved oxygen are located at 3.75 Å apart in apparent contradiction to the findings of Ref. 12. However, we can easily assume another conformation of the product state by reorienting the proton H_{2f} bound to Pi oxygen (see Fig. 8) towards GDP, and such rearrangement should not require noticeable energy expenses. The corresponding QM/MM minimization allowed us to obtain another construct for the products designated as PR2. The structure is shown in Figure 9.

This alternative configuration for the products is consistent with the findings of Pasqualato and Cherfills,¹² as can be also seen from a direct comparison of the crystal structure 1OIX¹² and the structure PR2 obtained in our modeling (see Fig. 10).

Remarkably, configuration PR2 is *lower in energy* than that of PR1: the energy of PR2 is -8.6 kcal/mol relative to the ES level and -1.8 kcal/mol relative to PR1. Therefore an observation of such species in experiments¹² can be easily explained; however, its appearance in our simulations is beyond the concept of substrate-

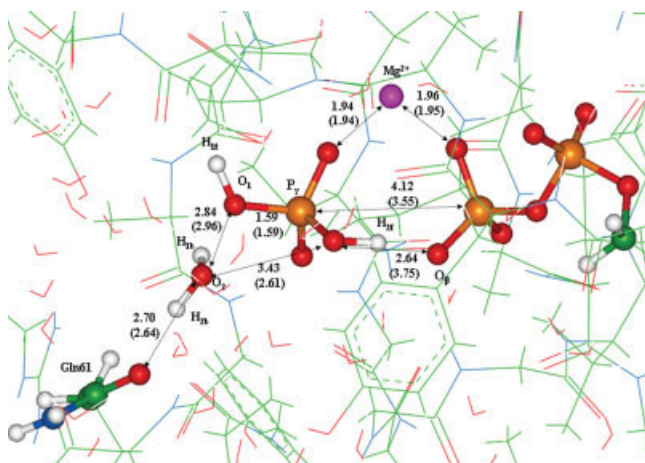


Fig. 9. Alternative geometry configuration of the reaction products (PR2) showing atoms of the quantum part in the ball and stick representation. Distances (in Å) without parentheses correspond to the PR2 structure and distances in parentheses correspond to the geometry of the previous structure PR1 (see Fig. 8). [Color figure can be viewed in the online issue, which is available at www.interscience.wiley.com.]

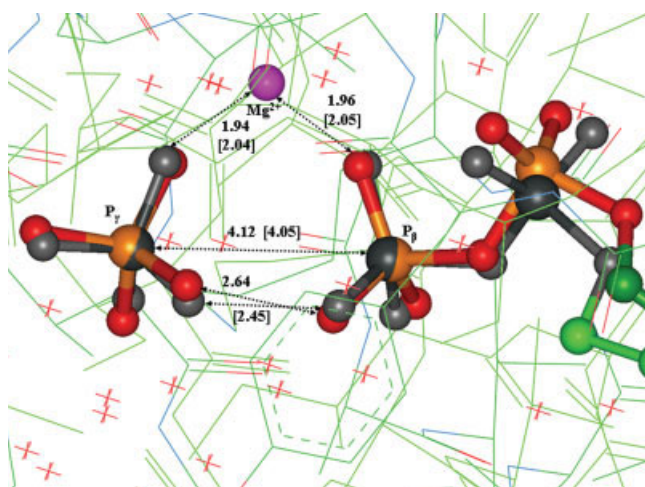


Fig. 10. Superposition of the arrangement GDP/Pi/Mg in the crystal structure 1OIX¹² and that in the computed structure PR2 (see Fig. 9). The black and grey colors refer to the atoms in the crystal. The distances between heavy atoms are specified in angstroms. The values in square brackets correspond to the 1OIX structure. [Color figure can be viewed in the online issue, which is available at www.interscience.wiley.com.]

assisted catalysis: the proton shared by Pi oxygen and the GDP cleaved oxygen, H_{2f}, is originally from another water molecule, but not from the lytic water molecule.

The anonymous Reviewer of the manuscript has drawn our attention to a possible role of the protonation status of a particular residue, His27, on the reaction mechanism. Figure 11 illustrates positions of His27 and of the active participants of the reaction in the crystal structure 1QRA.⁴⁷ Arrangement of these groups in another reference crystal structure 5P21⁴⁸ is essentially the same.

We performed several cycles of calculations of the reaction energy profiles, following the strategy described

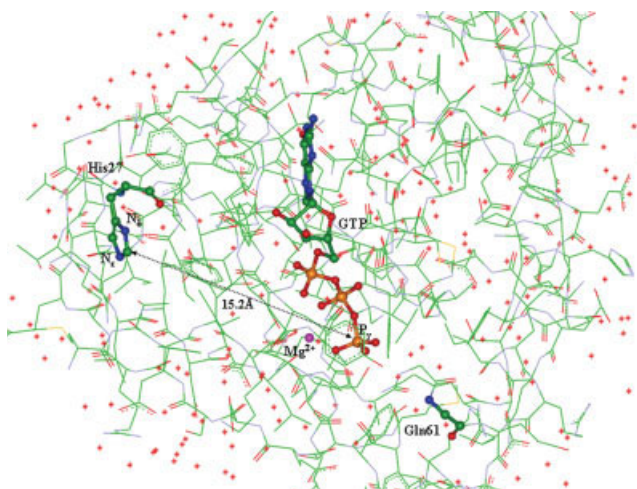


Fig. 11. The view of the crystal structure 1QRA showing His27 and the active participants of the reaction by balls and sticks. [Color figure can be viewed in the online issue, which is available at www.interscience.wiley.com.]

earlier, but including the side chain of His27 to the quantum part of the model QM/MM system. In the first series of calculations, His27 was assumed to be protonated on the N_ε position, while in the second series His27 was supposed to be unprotonated. In both cases equilibrium geometry configurations corresponding to the stationary points on potential energy surfaces (ES, TS1, INT1, INT2, TS3, PR2) were found practically the same as located previously with the His27 residue in the molecular mechanical subsystem. Computed relative energies at these stationary points also did not differ considerably from those obtained before: the largest deviations from the previous values (16.7, 8.1, -1.4, 7.5, and -8.6 kcal/mol for TS1, INT1, INT2, TS3, and PR2) amounted up to 0.2 kcal/mol. Therefore, the results of simulations do not seem sensitive to the protonation status of His27.

COMPARISON OF GTP HYDROLYSIS IN RAS AND RAS-GAP

We summarize in Table I the relative energies along the reaction profile obtained in the QM(SCF//LANL2DZdp)/MM(AMBER) approximation for the GTP hydrolysis in Ras (present work), for the methyl triphosphate hydrolysis in water,⁴⁰ for the GTP hydrolysis in Ras-GAP.³⁰ We note that it would be too naive to compare the computed highest reaction barriers (20 kcal/mol for water, 16.7 kcal/mol for Ras, and 10.5 kcal/mol for Ras-GAP) directly to the activation free energies estimated in Ref. 20 from the temperature dependence of the corresponding experimental rate constants (27.5 kcal/mol for water, 22.2 kcal/mol for Ras, and 15.9 kcal/mol for Ras-GAP). However, the experimentally-based difference in activation barriers of about 6 kcal/mol for the GTP hydrolysis in Ras and Ras-GAP is excellently repro-

TABLE I. Relative Energies (kcal/mol) Along the Reaction Profile for the Methyl triphosphate Hydrolysis in Water,⁴⁰ and for the GTP + H₂O Reaction in Ras and Ras-GAP³⁰ Estimated in the QM (SCF//LANL2DZdp)/MM(AMBER) Approximation^a

Structure	Water	Ras	Ras-GAP
Enzyme-substrate complex	0.0	0.0	0.0
Transition state for the P _γ -O _β bond cleavage (TS1)	20.0	16.7	4.4
Intermediate INT1	7.0	8.1	-2.0
Transition state for proton transfers (TS2/Ras)	—	≤10	—
Intermediate INT2	—	-1.4	—
Transition state for proton transfers (TS3/Ras or TS2/Ras-GAP ³⁰ or TS2/Water ⁴⁰)	14.1	7.5	10.5
Enzyme-product complex	-20.7	-6.8	-9.2
Enzyme-product complex (PR2/Ras)	—	-8.6	—

^aWe note that the relative energies shown in Fig. 6 of Ref. 30 refer to the values without MM contributions.

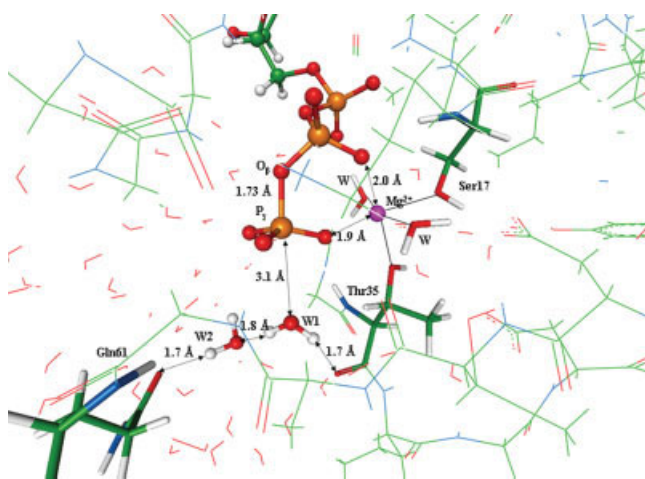


Fig. 12. The structure of ES complex in the Ras protein. [Color figure can be viewed in the online issue, which is available at www.interscience.wiley.com.]

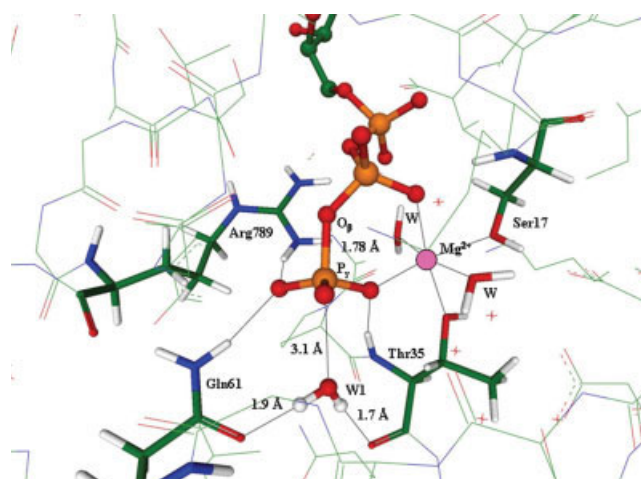


Fig. 13. The structure of ES complex in the Ras-GAP proteins.³⁰ [Color figure can be viewed in the online issue, which is available at www.interscience.wiley.com.]

duced in our simulations, as well as the energy effect of the hydrolysis reaction of about 8–9 kcal/mol.⁴⁹

There are some common and some distinctive features of the GTP hydrolysis in Ras and Ras-GAP. Figures 12 and 13, showing equilibrium geometry configurations of corresponding ES complexes in comparable perspectives, clearly illustrate that in both systems the reaction should begin with an in-line attack of the nucleophilic water molecule on γ -phosphate, as generally accepted.⁵⁰ One can see a remarkable similarity in the arrangements of reactants in both systems. A favorable position of the attacking water molecule (W1) towards the γ -phosphate group accomplished by the hydrogen bond network is supported by Thr35 and either Gln61 (Ras-GAP in Fig. 13) or another water molecule (Ras in Fig. 12). In this position the distance from the negatively charged oxygen atom of water to the positively charged γ -phosphorus of GTP (3.1 Å) is short enough for an efficient interaction of the reagents.

In Ras-GAP (see Fig. 13), the oxygen atoms of the γ -phosphate are oriented by Gln61 and Arg789, Thr35 and Mg²⁺, and also by Gly60 and Lys16 residues (not shown

in Figure 13). Such an arrangement provides immobility of the reagents, GTP + H₂O, in the pre-reactive state. Therefore, the immediate participants of reaction are left with the only one degree of freedom to approach each other, namely, along the O_β-P_γ-O_{w1} line. As a result, the O_β-P_γ bond is easily broken already at this stage leaving the attacking water almost unaltered. After separation of the γ -phosphate from GDP the stereochemical inversion of the PO₃ “umbrella” occurs, what allows the catalytic water to approach the metaphosphate PO₃⁻. Consequently, the molecular groups from Gln61, water, and PO₃⁻ form a cycle within which the protons are transferred until the inorganic phosphate H₂PO₄⁻ is created.³⁰

In pure Ras (see Fig. 12), the arginine finger of GAP is absent in the system; the oxygen atoms of the γ -phosphate are coordinated by Thr35, Mg²⁺, and Gly60 and Lys16 (see Fig. 2), and water molecules instead of Gln61 and Arg789 in Ras-GAP. Because of the latter, the reagents are more mobile than those in Ras-GAP. The O_β-P_γ bond is broken already at the first stage of

the process, again leaving the attacking water almost unaltered, but the corresponding activation energy is considerably higher (Table I). Again, after separation of the γ -phosphate from GDP the stereochemical inversion of the PO_3 occurs, what allows the catalytic water to approach the metaphosphate PO_3^- . The molecular groups from Gln61, water molecules, and PO_3^- participate in proton transfers until the inorganic phosphate H_2PO_4^- is created.

These considerations allow us to rationalize why the first stage of the hydrolysis reaction, i.e. the $\text{P}_\gamma\text{--O}_\beta$ bond cleavage, proceeds with noticeably different activation barriers in Ras and Ras-GAP.

In Figure 14 we compare the atomic charges on the phosphate part of GTP in Ras and Ras-GAP obtained in QM/MM calculations for ES complexes following the natural bond orbital (NBO) analysis.⁵¹ The values of the charges for GTP in Ras are well consistent with those reported by Klähn et al.²⁸ Remarkably, no considerable

differences in charge distributions are noticed for two protein systems, Ras and Ras-GAP.

In Table II we compare electronic properties of the bridging P–O bonds of GTP captured in the ES complexes with either Ras or Ras-GAP (see Fig. 14 for atomic labeling). To compute such localized characteristics as orbital energies of bonding $\sigma(\text{P--O})$ or antibonding $\sigma^*(\text{P--O})$ orbitals and their occupation numbers, we apply the NBO analysis⁵¹ for the QM/MM(EFP) electronic densities. We do not show in Table II the occupation numbers of bonding orbitals, since all of them are practically the same, 1.97–1.98.

Apparently, localized properties of the $\text{P}_\gamma\text{--O}_\beta$ bond are noticeably different from those of other bridging P–O bonds, indicating that this bond is the weakest in the molecule captured by the proteins. We note in passing that according to these estimates, the next bond which is likely to be cleaved is the $\text{P}_\alpha\text{--O}_\alpha$ bond. However, from quantitative side, the differences between orbital energies and occupation numbers of $\sigma^*(\text{P}_\gamma\text{--O}_\beta)$ in Ras and in Ras-GAP do not seem substantial. The only exception is the energy required to promote the electron from $\sigma(\text{P}_\gamma\text{--O}_\beta)$ to $\sigma^*(\text{P}_\gamma\text{--O}_\beta)$, which should lead to the cleavage of this bond: 1.52 a.u. in Ras versus 1.43 a.u. in Ras-GAP; this is a substantial energy difference, especially if converted to other energy units, e.g., more than 50 kcal/mol.

It is interesting that the positive charge on the arginine finger (Arg789) does not seem to have a decisive effect on electronic properties of GTP captured by Ras-GAP. We recomputed the values for atomic charges, orbital energies, and occupation numbers for a model system, in which the true arginine side chain ($\dots\text{--CH}_2\text{--NH--C}(\text{NH}_2)_2^+$) was replaced by an artificial construct $\dots\text{--CH}_2\text{--NH--N}(\text{NH}_2)_2$ bearing zero charge. The only noticeable differences observed in such simulations relative to the items shown in Figure 13 and Table II referred to the values of orbital energies, for example, $\varepsilon(\text{P}_\gamma\text{--O}_\beta)$ changed to -0.64 a.u., and $\varepsilon^*(\text{P}_\gamma\text{--O}_\beta)$ changed to 0.78 a.u., keeping the energy gap ($\varepsilon^* - \varepsilon$) essentially the same as before. In summary, localized electronic properties of the $\text{P}_\alpha\text{--O}_\alpha$ bond in Ras are modified by

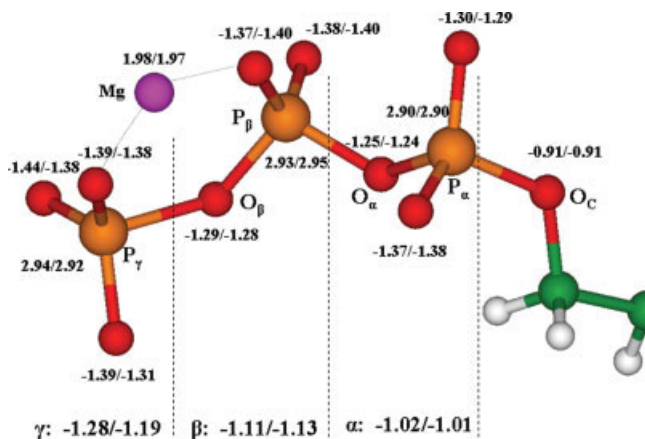


Fig. 14. Atomic charges on the phosphate part of GTP in Ras and Ras-GAP³⁰ obtained in QM/MM calculations following the NBO analysis.⁵¹ First items before the slash sign refer to Ras and second items after the slash sign correspond to Ras-GAP. The total charges on the $\text{P}_\gamma\text{O}_3$, P_βO_3 , and $\text{P}_\alpha\text{O}_3$ groups are specified in the bottom of the graph. [Color figure can be viewed in the online issue, which is available at www.interscience.wiley.com.]

TABLE II. Computed Properties of the Bridging P–O Bonds of GTP Captured in the Enzyme–Substrate Complexes with Either Ras or Ras-GAP

Property	Protein	$\text{P}_\gamma\text{--O}_\beta$	$\text{P}_\beta\text{--O}_\beta$	$\text{P}_\beta\text{--O}_\alpha$	$\text{P}_\alpha\text{--O}_\alpha$	$\text{P}_\alpha\text{--O}_\gamma$
Equilibrium distance (\AA)	Ras	1.73	1.59	1.60	1.66	1.59
	Ras-GAP	1.78	1.56	1.62	1.65	1.61
Occupation number of antibonding orbital $\sigma^*(\text{P--O})$	Ras	0.20	0.14	0.15	0.18	0.14
	Ras-GAP	0.23	0.12	0.14	0.17	0.15
Orbital energy of bonding orbital $\sigma(\text{P--O})$, ε (atomic units)	Ras	-0.75	-0.87	-0.85	-0.79	-0.84
	Ras-GAP	-0.76	-0.94	-0.91	-0.88	-0.89
Orbital energy of antibonding orbital $\sigma^*(\text{P--O})$, ε^* (atomic units)	Ras	0.77	1.00	0.98	0.87	0.97
	Ras-GAP	0.67	1.01	0.88	0.83	0.86
Energy difference $\varepsilon^* - \varepsilon$ (atomic units)	Ras	1.52	1.87	1.83	1.66	1.81
	Ras-GAP	1.43	1.95	1.79	1.71	1.75

Equilibrium distances refer to the respective minima of the QM/MM energy. Occupation numbers and orbital energies are estimated following the NBO analysis.⁵¹

GAP in such a manner that it is getting even weaker in the protein environment.

An assumption of another mechanism in which a penta-coordinated phosphorus intermediate plays a central role was also tested for the pure Ras molecular model in the same fashion like in our previous works.^{29,30} The same strategy was applied as in Ref. 30. The structure at the top of the potential barrier resembled that shown in Figure 7 of Ref. 30 and the corresponding activation barrier was estimated as greater than 30 kcal/mol.

CONCLUSIONS

Our QM/MM simulations described in this paper and previously^{29,30} result in a conclusion that the low-energy reaction path for the GTP hydrolysis connecting the reagents, GTP + H₂O, and products, GDP + H₂PO₄⁻, is consistent with the two-step process. When the unprotonated substrate, GTP, is trapped in a protein environment, the O_β–P_γ bond is getting weaker, what can be traced by an elongation of the corresponding equilibrium O_β–P_γ distance in the ES complex and by increased occupation numbers of the corresponding localized anti-bonding orbital. Consequently, fairly low activation energies are required at the first step to cleave this bond and to separate the γ-phosphate group from GDP: 16.7 kcal/mol for Ras and 4.4 kcal/mol for Ras-GAP counted from the ES complex energy level. Equilibrium geometry configurations of the reaction intermediates created after the first transition state corresponds to the metaphosphate anion PO₃⁻ stereochemically inverted relative to the structure of the γ-phosphate group in GTP. Both species, PO₃⁻ and lytic water H₂O, are involved in the hydrogen bond network with the neighboring molecular groups, including the key residue Gln61 in both cases, Ras and Ras-GAP. To complete the reaction and to arrive to the product H₂PO₄⁻, the cycle of proton transfers via the hydrogen bond network should occur at the second step. The corresponding energy barriers are estimated as 7.5 kcal/mol for Ras and 10.5 kcal/mol for Ras-GAP counted from the ES complex energy level.

The results of the modeling described in this and in previous paper³⁰ do not contradict information gained in structural studies.^{12,47,48,52,53} Moreover, the theoretical conclusions confirm some hypotheses about the reaction mechanism considered in these studies. Our QM/MM calculations described in this work for Ras, and in previous papers for Ras-GAP³⁰ and for water⁴⁰ performed at the same computational level present a brute force theoretical approach allowing one to analyze minimum energy path connecting reagents and products. These data benefit knowledge of the details of reaction mechanisms irrespective of precise classification of the latter.

These results help to develop better understanding of the anticatalytic effect of cancer causing mutations of Ras at position 61, which has been debated in recent years. Our calculations provide strong support to the

direct involvement of Gln61 in the process of GTP hydrolysis by Ras and by Ras-GAP.

ACKNOWLEDGMENTS

BLG and AVN thank Prof. A. Warshel for critical discussions and valuable suggestions. AVN is grateful to Prof. R. Goody and Prof. A. Wittinghofer for stimulating talks on the subject. We thank the staff and administration of the Advanced Biomedical Computing Center for their support of this project. The content of this publication does not necessarily reflect the views or policies of the Department of Health and Human Services, nor does mention of trade names, commercial products, or organization imply endorsement by the U.S. Government.

REFERENCES

- Bourne HR, Sanders DA, McCormick F. The GTPase superfamily: conserved structure and molecular mechanism. *Nature* 1991;349:117–127.
- Maegley KA, Admiraal SJ, Herschlag D. Ras-catalyzed hydrolysis of GTP: a new perspective from model studies. *Proc Natl Acad Sci USA* 1996;93:8160–8166.
- Sprang SR. G protein mechanisms: insight from structural analysis. *Annu Rev Biochem* 1997;66:639–678.
- Mildvan AS. Mechanisms of signaling and related enzymes. *Proteins: Struct Funct Genet* 1997;29:401–416.
- Sprang SR. GAP into the breach. *Science* 1997;277:329, 330.
- Bourne HR. G proteins: the arginine finger strikes again. *Nature* 1997;389:673, 674.
- Scheffzek K, Ahmadian MR, Wittinghofer A. GTPase-activating proteins: helping hands to complement an active site. *Trends Biochem Sci* 1998;23:257–262.
- Vetter IR, Wittinghofer A. Signal transduction. The guanine nucleotide-binding switch in three dimensions. *Science* 2001;294:1299–1304.
- Kosloff M, Selinger Z. Substrate assisted catalysis—application to G proteins. *Trends Biochem Sci* 2001;26:257–262.
- Li G, Zhang XC. GTP hydrolysis mechanism of Ras-like GTPases. *J Mol Biol* 2004;340:921–932.
- Wittinghofer A. Phosphoryl transfer in Ras proteins, conclusive or elusive? *Trends Biochem Sci* 2006;31:20–23.
- Pasqualato S, Cherfils J. Crystallographic evidence for substrate-assisted GTP hydrolysis by a small GTP binding protein. *Structure* 2005;13:533–540.
- Åqvist J, Kolmodin K, Florian J, Warshel A. Mechanistic alternatives in phosphate monoester hydrolysis: what conclusions can be drawn from available experimental data? *Chem Biol* 1999;6:R71–R80.
- Langen R, Schweins T, Warshel A. On the mechanism of guanosine triphosphate hydrolysis in ras p21 proteins. *Biochemistry* 1992;31:8691–8696.
- Schweins T, Langen R, Warshel A. Why have mutagenesis studies not located the general base in ras p21. *Nat Struct Biol* 1994;1:476–484.
- Schweins T, Warshel A. Mechanistic analysis of the observed linear free energy relationships in p21^{ras} and related systems. *Biochemistry* 1996;35:14232–14243.
- Schweins T, Geyer M, Kalbitzer HR, Wittinghofer A, Warshel A. Linear free energy relationships in the intrinsic and GTPase activating protein-stimulated guanosine 5'-triphosphate hydrolysis of p21^{ras}. *Biochemistry* 1996;35:14225–14231.
- Florian J, Warshel A. Phosphate ester hydrolysis in aqueous solution: associative versus dissociative mechanisms. *J Phys Chem B* 1998;102:719–734.
- Glennon TM, Villa J, Warshel A. How does GAP catalyze the GTP reaction of Ras? A computer simulation study. *Biochemistry* 2000;39:9641–9651.
- Shurki A, Warshel A. Why does the Ras switch “break” by oncogenic mutations? *Proteins* 2004;55:1–10.

21. Warshel A, Parson WW. Dynamics of biochemical and biophysical reactions: insight from computer simulations. *Q Rev Biophys* 2001;34:563–679.
22. Lee FS, Chu ZT, Warshel A. Microscopic and semimicroscopic calculations of electrostatic energies in proteins by the POLARIS and ENZYMI programs. *J Comput Chem* 1993;14:161–185.
23. Futatsugi N, Hata M, Hoshino T, Tsuda M. Ab initio study of the role of lysine 16 for the molecular switching mechanism of ras protein p21. *Biophys J* 1999;77:3287–3292.
24. Futatsugi N, Tsuda M. Molecular dynamics simulations of Gly-12 → Val mutant of p21^{ras}: dynamic inhibition mechanism. *Biophys J* 2001;81:3483–3488.
25. Katagiri D, Hata M, Itoh T, Neya S, Hoshino T. Atomic-scale mechanism of the GTP → GDP hydrolysis reaction by the Giα1 protein. *J Phys Chem B* 2003;107:3278–3283.
26. Cavalli A, Carloni P. Enzymatic GTP hydrolysis: insights from an ab initio molecular dynamics. *J Am Chem Soc* 2002;124:3763–3768.
27. Klähn M, Schlitter J, Gerwert K. Theoretical IR spectroscopy based on QM/MM calculations provides changes in charge distribution, bond lengths, and bond angles of the GTP ligand induced by the Ras-protein. *Biophys J* 2005;88:3829–3844.
28. Soares TA, Miller JN, Straatsma TP. Revisiting the structural flexibility of the complex p21^{ras}-GTP: the catalytic conformation of the molecular switch II. *Proteins: Struct Funct Genet* 2001;45:297–312.
29. Topol IA, Cachau RE, Nemukhin AV, Grigorenko BL, Burt SK. Quantum chemical modeling of the GTP hydrolysis by the Ras-GAP protein complex. *Biochem Biophys Acta* 2004;1700:125–136.
30. Grigorenko BL, Nemukhin AV, Topol IA, Cachau RE, Burt SK. QM/MM modeling the Ras-GAP catalyzed hydrolysis of guanosine triphosphate. *Proteins: Struct Funct Bioinformatics* 2005;60:495–503.
31. Gordon MS, Freitag MA, Bandyopadhyay P, Jensen JH, Kairys V, Stevens WJ. The effective fragment potential method: a QM-based MM approach to modeling environmental effects in Chemistry. *J Phys Chem A* 2002;105:293–307.
32. Nemukhin AV, Grigorenko BL, Bochenkova AV, Topol IA, Burt SK. A QM/MM approach with effective fragment potentials applied to the dipeptide-water structures. *J Mol Struct (THEOCHEM)* 2002;581:167–175.
33. Grigorenko BL, Nemukhin AV, Topol IA, Burt SK. Modeling of biomolecular systems with the quantum mechanical and molecular mechanical method based on the effective fragment potential technique: proposal of flexible fragments. *J Phys Chem A* 2002;106:10663–10672.
34. Nemukhin AV, Grigorenko BL, Topol IA, Burt SK. Flexible effective fragment QM/MM method: validation through the challenging tests. *J Comput Chem* 2003;24:1410–1420.
35. Nemukhin AV, Grigorenko BL, Rogov AV, Topol IA, Burt SK. Modeling of the serine protease prototype reactions with the flexible effective fragment potential QM/MM method. *Theor Chem Acc* 2004;111:36–48.
36. Warshel A, Levitt M. Theoretical studies of enzymatic reactions: dielectric, electrostatic and steric stabilization of the carbonium ion in the reaction of lysozyme. *J Mol Biol* 1976;103:227–249.
37. Field MJ, Bash PA, Karplus MA. Combined ab initio quantum mechanical and molecular mechanical method for carrying out simulations on complex molecular systems: applications to the CH₃Cl⁺ Cl⁻ exchange reaction and gas phase protonation of polyethers. *J Comput Chem* 1990;11:700–733.
38. Gao JL, Xia XF. A priori evaluation of aqueous polarization effects through Monte Carlo QM/MM simulations. *Science* 1992;258:631–635.
39. Klähn M, Braun-Sand S, Rosta E, Warshel A. On possible pitfalls in ab initio quantum mechanics/molecular mechanics minimization approach for studies of enzymatic reactions. *J Phys Chem B* 2005;109:15645–15650.
40. Grigorenko BL, Rogov AV, Nemukhin AV. On the mechanism of triphosphate hydrolysis in aqueous solution: QM/MM simulations in water clusters. *J Phys Chem B* 2006;110:4407–4412.
41. Cornell WD, Cieplak P, Bayly CI, Gould IR, Merz KM, Ferguson DM, Spellmeyer DC, Fox T, Caldwell JW, Kollman PA. A second generation force field for the simulation of proteins, nuclear acids, and organic molecules. *J Am Chem Soc* 1995;117:5179–5197.
42. Schmidt MW, Baldrige KK, Boatz JA, Elbert ST, Gordon MS, Jensen JH, Koseki S, Matsunaga N, Nguyen KA, Su SJ, Windus TL, Dupuis M, Montgomery JA. The general atomic and molecular electronic structure system. *J Comput Chem* 1993;14:1347–1356.
43. Nemukhin AV, Grigorenko BL, Granovsky AA. Molecular modeling with the PC GAMESS system: form diatomic molecules to enzymes. *Moscow State Univ Res Bull Khimia* 2004;45:75–102.
44. Ponder JW, Richards FM. An efficient Newton-like method for molecular mechanics energy minimization of large molecules. *J Comput Chem* 1987;8:1016–1026.
45. Dunning TH, Hay PJ. Gaussian basis sets for molecular calculations. In: Schaefer HF, editor. *Methods of electronic structure theory*, Vol. 3. New York: Plenum; 1977. pp. 1–27.
46. Berman HM, Westbrook J, Feng Z, Gilliland G, Bhat TN, Weissig H, Shindyalov IN, Bourne PE. The Protein Data Bank. *Nucleic Acids Res* 2000;28:235–242.
47. Scheidig AJ, Burmester C, Goody RS. The pre-hydrolysis state of p21^{ras} in complex with GTP: new insights into the role of water molecules in the GTP hydrolysis reaction of ras-like proteins. *Structure* 1999;7:1311–1324.
48. Pai EF, Krengel U, Petsko GA, Goody RS, Kabsch W, Wittinghofer A. Refined crystal structure of the triphosphate conformation of H-ras p21 at 1.35 Å resolution: implications for the mechanism of GTP hydrolysis. *EMBO J* 1990;9:2351–2359.
49. Kötting C, Gerwert K. Time-resolved FTIR studies provide activation free energy, activation enthalpy and activation entropy for GTPase reactions. *Chem Phys* 2004;307:227–232.
50. Feuerstein J, Goody RS, Webb MR. The mechanism of guanosine nucleotide hydrolysis by p21 c-Ha-ras. The stereochemical course of the GTPase reaction. *J Biol Chem* 1989;264:6188–6190.
51. Reed AE, Curtiss LA, Weinhold F. Intermolecular interactions from a natural bond orbital, donor-acceptor viewpoint. *Chem Rev* 1988;88:899–926.
52. Sondek J, Lambright DG, Noel JP, Hamm HE, Sigler PB. GTPase mechanism of Gproteins from the 1.7-Å crystal structure of transducin α GDP AlF₄⁻. *Nature* 1994;372:276–279.
53. Scheffzek K, Ahmadian MR, Kabsch W, Wiesmüller L, Lautwein A, Schmitz F, Wittinghofer A. The Ras-RasGAP complex: structural basis for GTPase activation and its loss in oncogenic Ras mutants. *Science* 1997;277:333–338.